



THE UNIVERSITY *of* EDINBURGH

Edinburgh Research Explorer

Chronic pleuropulmonary fibrosis and elastosis of aged donkeys: similarities to human pleuroparenchymal fibroelastosis

Citation for published version:

Miele, A, Dhaliwal, K, Du Toit, N, Murchison, JT, Dhaliwal, C, Brooks, H, Smith, SH, Hirani, N, Schwarz, T, Haslett, C, Wallace, W & McGorum, BC 2014, 'Chronic pleuropulmonary fibrosis and elastosis of aged donkeys: similarities to human pleuroparenchymal fibroelastosis' *Chest*, vol. 145, no. 6, pp. 1325-32. DOI: 10.1378/chest.13-1306

Digital Object Identifier (DOI):

[10.1378/chest.13-1306](https://doi.org/10.1378/chest.13-1306)

Link:

[Link to publication record in Edinburgh Research Explorer](#)

Document Version:

Early version, also known as pre-print

Published In:

Chest

General rights

Copyright for the publications made accessible via the Edinburgh Research Explorer is retained by the author(s) and / or other copyright owners and it is a condition of accessing these publications that users recognise and abide by the legal requirements associated with these rights.

Take down policy

The University of Edinburgh has made every reasonable effort to ensure that Edinburgh Research Explorer content complies with UK legislation. If you believe that the public display of this file breaches copyright please contact openaccess@ed.ac.uk providing details, and we will remove access to the work immediately and investigate your claim.



Chronic pleuropulmonary fibrosis and elastosis of aged donkeys - similarities to human pleuroparenchymal fibroelastosis (PPFE)

Amy Miele^{1}, BVM&S; Kevin Dhaliwal^{1*}, MBChB PhD; Nicole Du Toit², BVSc PhD; John T Murchison³, MBChB PhD; Catharine Dhaliwal⁴, MBChB PhD; Harriet Brooks², BVetMed PhD; Sionagh H Smith⁵, BVMS PhD; Nik Hirani¹, MBChB PhD; Tobias Schwarz⁵, MA Dr.med.vet; Chris Haslett¹, MBChB; William A Wallace^{*4}, MBChB PhD and Bruce McGorum^{*5}, BVM&S PhD*

MRC Centre for Inflammation Research¹, Queen's Medical Research Institute, University of Edinburgh, Edinburgh.

The Donkey Sanctuary², Sidmouth, Devon.

Departments of Radiology³ and Pathology⁴, New Edinburgh Royal Infirmary, Edinburgh.

Royal (Dick) School of Veterinary Studies and Roslin Institute⁵, University of Edinburgh, Edinburgh.

*** contributed equally**

Corresponding Author: Amy Miele, Room C2.17, MRC Centre for Inflammation Research, Queen's Medical Research Institute, 47 Little France Crescent, Edinburgh, EH164TJ.

Tel: 0131 242 6551, Email: a.c.miele@sms.ed.ac.uk

Conflict of Interest: The authors have no conflict of interest to declare.

Funding: MRC

Prior abstract publication: BSAS annual conference, Nottingham, 17th April 2013

Abbreviations

DPF: donkey pulmonary fibrosis

AsHV: asinine herpesvirus

α -SMA: alpha smooth muscle actin

ATS: American Thoracic Society

DNA: deoxyribonucleic acid

EMPF: equine multinodular pulmonary fibrosis

EVG: Elastic Van Gieson

H&E: haematoxylin and eosin

HRCT: high resolution computed tomography

PCR: polymerase chain reaction

PPFE: pleuroparenchymal fibroelastosis

Abstract

Background: Donkey Pulmonary Fibrosis (DPF) is a spontaneous syndrome of aged donkeys with high prevalence (35%). No previous detailed characterisation of DPF has been performed. We sought to determine the similarities of DPF to recognised patterns of human pulmonary fibrosis.

Methods: Whole lungs were collected from 32 aged donkeys at routine necropsy. Gross examination revealed pulmonary fibrosis in 19 donkeys (DPF cases), while 13 (controls) had grossly normal lungs. Eighteen whole inflated *ex vivo* lungs (11 DPF, 7 controls) were imaged with high resolution computed tomography (HRCT), while the remainder were sectioned and photographed. Tissue samples were collected from all lungs for histopathological evaluation using a standardised protocol. HRCT images and histology sections were reviewed independently and blindly. Lung tissue was analysed for herpes virus, fungal hyphae, mycobacteria and dust content.

Results: Ten of 19 DPF lungs were categorised as being ‘consistent with’ pleuroparenchymal fibroelastosis (PPFE) according to previously defined histological and imaging criteria. All 10 PPFE-like lungs had marked pleural and subpleural fibrosis, predominantly within the upper lung zone, with accompanying intra-alveolar fibrosis and elastosis. Asinine herpesvirus (AsHV) was ubiquitously expressed within control and DPF lung tissue. No other aetiological agents were identified.

Conclusions: Many cases of DPF share key pathological and imaging features with human PPFE, a rare interstitial pneumonia. Consequently, further study of DPF may help elucidate the aetiopathogenesis of human PPFE.

Introduction

Pulmonary fibrosis represents the endpoint of many diseases and is characterised by excessive and irreversible deposition of extracellular matrix in the lung parenchyma, leading to compromised ventilation and organ dysfunction. Despite considerable research, many fibrotic lung diseases remain elusive in terms of aetiology, pathogenesis and treatment (1). Progress is hindered by the lack of a translatable animal model with durable and persistent fibrosis (2).

The term idiopathic pleuroparenchymal fibroelastosis (PPFE) was appointed by the authors of a case study in 2004 to describe a novel clinicopathological entity which did not fall within the 2002 American Thoracic Society (ATS) consensus classifications of idiopathic interstitial pneumonias (3). Authors described a predominantly upper zone distribution of pleural and subpleural fibrosis with elastosis and proposed that previous reports of idiopathic pulmonary fibrosis of upper lung lobes were consistent with PPFE (3). PPFE was subsequently included in the recent ATS/European Respiratory Society Statement on the Update of the International Multidisciplinary Classification of the Idiopathic Interstitial Pneumonias (2013), in the category of rare idiopathic interstitial pneumonias (4). While PPFE is regarded as usually idiopathic, it has been linked with connective tissue diseases, genetic predisposition or autoimmunity following organ transplant (3-5). Reddy *et al* (2012) suggested that repeated inflammatory damage following recurrent infections in predisposed individuals could lead to PPFE and that airway centred injury could be key to disease pathogenesis (5).

Donkey Pulmonary Fibrosis (DPF) is a syndrome that is also sparsely documented, yet a prevalence of 35% at routine necropsy was reported in a UK cohort (6). Very little is known about this chronic, potentially debilitating and currently untreatable idiopathic condition. To test our hypothesis that many cases of DPF share the key pathological and imaging

characteristics of PPFE, we performed the most comprehensive systematic characterisation of DPF to date.

Materials and Methods

Tissue collection and processing

Whole lungs were collected from 32 aged donkeys during routine necropsy at two UK donkey sanctuaries between June 2009 and January 2013 . Nineteen ‘DPF’ lungs were selected because of grossly visible fibrosis, while 13 grossly unaffected ‘control’ lungs were selected at random. All lungs were manually inflated, the tracheas clamped and gross images photographed. Tissue samples were collected from each lung into 10% buffered formalin, essentially as described previously (7), before undergoing routine processing to paraffin blocks. Sections were stained with haematoxylin and eosin (H&E), Elastic Van Gieson (EVG) and Masson’s Trichrome. Tissue samples from 8 lungs (4 DPF, 4 controls) were collected into RNeasy (Qiagen) for deoxyribonucleic acid (DNA) extraction and subsequent polymerase chain reaction (PCR). As this study utilised only *ex vivo* tissue collected at routine necropsy, licensing on ethical and humane grounds was not required.

Histology

Histology sections were reviewed independently and blindly by 3 medical and veterinary pathologists with experience in lung disease. Subsequent to the recognition that the changes observed resembled those of human PPFE, the histological features were categorised as being ‘consistent with’ or ‘inconsistent with’ PPFE according to criteria described by Reddy *et al*, 2012 (5). Cases were categorised as ‘consistent with’ PPFE on histology if (a) there was pleural thickening with associated subpleural intra-alveolar fibrosis and alveolar septal elastosis, or (b) intra-alveolar fibrosis was present but either not associated with pleural

fibrosis, not predominantly subpleural or not in a dorsal lobe sample. ‘Inconsistent with’ PPFE was assigned to lungs that lacked the aforementioned features.

HRCT and digital photography

Eighteen whole inflated *ex vivo* lungs (11 DPF, 7 control) were imaged using HRCT (Toshiba Aquilon One Toshiba Medical Systems, Tokyo, Japan or Siemens Somatom Volume Zoom, Siemens Aktiengesellschaft, Munich, Germany). The remaining lungs (8 DPF, 6 control) were systematically sectioned transversely and photographed digitally. All images were reviewed independently and blindly by an expert radiologist and were categorised as ‘consistent with’ or ‘inconsistent with’ PPFE according to criteria described previously (5). Cases were categorised as ‘consistent with’ PPFE if there was (a) pleural thickening with associated subpleural fibrosis predominantly in the dorsal lung, or (b) dorsal lung pleural thickening and associated subpleural fibrosis but the distribution of fibrosis was not concentrated in the dorsal lung or there was evidence of coexistent lung disease elsewhere. ‘Inconsistent with’ PPFE was assigned to lungs that lacked the aforementioned features. Overall, cases were assigned as ‘PPFE-like’ only if categorised as ‘consistent with’ PPFE on both imaging and histology.

PCR for herpesviral polymerase

Eight lung samples (4 DPF, 4 control) collected into RNAlater were processed using an AllPrep DNA/RNA Mini Kit (Qiagen) according to manufacturer’s instructions. For investigation of the presence of herpesvirus, a region of the herpesvirus DNA polymerase gene was amplified using 100ng of DNA per reaction with two sets of nested degenerate primers as previously described (8). PCR products were cloned into the TOPO®TA vector

(Invitrogen), sequenced (Genepool, Edinburgh) and Blastn (2.6.2) used to align derived sequences against known herpesvirus sequences.

Special staining

Lung sections in which there was granulomatous inflammation were stained for acid fast bacteria using a standard Ziehl-Neelsen stain and for fungal hyphae using Grocott's methenamine silver and Periodic acid-Schiff stains.

X-ray diffraction

Formalin fixed wet lung tissue samples from 4 DPF *ex vivo* lungs were pooled, digested in KOH and then prepared for mineral particle analysis under transmission electron microscopy at a magnification of 20,000 and for energy dispersive x-ray analysis. The mass of dust per gram of dry lung tissue was established. Both fibrous and non-fibrous particles were counted and typed.

Results

Ages of DPF (median 31 years, range 14-53) and control (28 years, 4-36) donkeys at necropsy were not significantly different (Mann Whitney, $p > 0.05$). The typical donkey lifespan is 30 years. Donkeys comprised 12 neutered males and 20 females.

Ten of 19 DPF lungs were categorised as being 'PPFE-like', having features 'consistent with' PPFE on both pathology (Table 1) and imaging (7 on HRCT; 3 on photographed images of sectioned lungs). All 10 'PPFE-like' lungs had grossly visible visceral pleural fibrosis on the dorsal /costal surface with no involvement of the parietal pleura. This was characterised by multifocal to coalescing vermiform cream/grey lesions that caused visible restriction to pleural expansion on manual lung inflation (Figure 1). As donkeys are quadrupeds, the dorsal

lung equates to the human upper zone. Histologically, all 10 ‘PPFE-like’ lungs had dorsal pleural and subpleural fibrosis with subpleural intra-alveolar fibrosis and elastosis evident on EVG stained sections (Figure 2A-D). Spatial heterogeneity was a consistent feature, often with a sharp interface between fibrotic and adjacent ‘normal’ tissue (Figure 2E). Other common features (Table 2) included septal and bronchiolocentric fibrosis, lymphoplasmacytic bronchiolitis, granulomatous inflammation and vascular remodelling within areas of fibrosis (Figure 2F-H). Honeycombing and fibroblastic foci were not detected, although myofibroblasts were demonstrated within fibrotic lesions using α -smooth muscle actin immunohistochemistry (supplemental e-Figure 2).

All 7 ‘PPFE-like’ lungs which had undergone HRCT had pleuroparenchymal thickening (max 5-32mm) of the dorsal lung lobes with associated subpleural consolidation consistent with established fibrosis. The consolidation extended from the subpleural region along parenchymal bands (Figure 3). In 2/7 lungs the fibrosis was relatively superficial and confined solely to uppermost zones of the dorsal lung surface. The other 5 cases had consolidation extending along parenchymal bands into mid and ventral zones, and often radiating out to surround adjacent bronchi. Features of coexistent disease identified on HRCT included primary bronchiectasis and “ground glass” opacity. Traction bronchiectasis was present to varying degrees in all 7 cases (Table 2). “Ground glass” change was a feature of 4/7 lungs, although some of this was attributed to collapse of dependent parenchyma in the inflated *ex vivo* tissue, a feature also noted in 3/7 control lungs.

All 9 DPF lungs classified as ‘inconsistent with’ PPFE on histology, had pleural, subpleural or septal fibrosis in at least one section. In 4/9 lungs the fibrosis was focussed around alveolar walls, with similarities to a non-specific interstitial pneumonia-type pattern (Figure 2I-J).

Importantly, all 9 lungs lacked the intra-alveolar fibrosis previously reported to be a feature of PPFE (5), but the majority (7/9) had marked intra-alveolar mononuclear cell infiltrates with fibrin deposition.

Four of 19 lungs were classified as ‘inconsistent with’ PPFE on imaging (HRCT n=2; photographic n=2). Two of these had small amounts of dorsal pleural and subpleural fibrosis that was either asymmetrical or considered not to be a predominant feature. One had a predominantly ventral distribution of fibrosis, while the other showed diffuse “ground glass” opacity (Figure 4).

Acid fast bacteria and fungi were not identified with special staining. Herpesviral sequences were identified in 6 of 8 lung homogenates, with 5 mapping to AsHV-5 and 1 to AsHV- 4. X-ray diffraction analysis revealed a dust burden of 6.98mg/g dry lung. Small numbers of fibrous particles were identified: talc 0.28 and silica 0.14 million fibres/g dry lung. The percentages of non-fibrous particles were calcium silicate 95, potassium silicate 2, kaolin 1, muscovite 1 and silica 1. No asbestos fibres were found.

Discussion

This is the most comprehensive study of a spontaneous large animal model of pulmonary fibrosis to date. While the donkey may seem an implausible candidate with which to share pathological features of pulmonary disease, of all the domestic species, the subgross anatomy of the equine lung and visceral pleura most closely resembles that of humans (9).

DPF was first reported as a common incidental necropsy finding of donkeys resident at a donkey sanctuary in 2001 (10). Reported gross and histopathological findings were consistent with those for the current study, including a wide spectrum of pleural, subpleural and septal

fibrosis extending into the interstitium of dorsal lung fields, with more diffuse and ventral changes in severely affected cases. Peribronchial cuffing and multifocal aggregates of mononuclear cells were also described (10). However, the presence of intra-alveolar fibrosis and alveolar septal elastosis was not reported, probably because these features are less striking in the absence of EVG staining. It should be noted that fibroblastic foci and honeycombing are not features of DPF.

In this study, over 50% of donkeys with DPF shared key imaging and pathological characteristics of human PPFE. DPF lungs were classified as ‘PPFE-like’ only if they had features considered ‘consistent with’ PPFE (3) on both histology and imaging. In this respect, a greater proportion of DPF lungs were classified as ‘consistent with’ PPFE on HRCT (82%) compared to histology (58%). It is possible that some of the 9 lungs classified as ‘inconsistent with’ PPFE on histology represent an earlier stage of ‘PPFE-like’ disease. Seven of these had intra-alveolar mononuclear inflammatory infiltrates with organising intra-alveolar fibrin which is a likely prelude to intra-alveolar fibrosis (Figure 2I). Furthermore, the marked spatial heterogeneity in extent and pattern of fibrosis meant that ‘PPFE-like’ pathology may have been missed as a result of unrepresentative sampling in some cases.

Imaging of ‘PPFE-like’ lungs indicated that, although all had the characteristic predominantly dorsal distribution of lesions, 7/10 lungs also had pleural and subpleural fibrosis in the mid and ventral pulmonary parenchyma. Similarly, Reddy *et al*, 2012 reported that 6/12 PPFE lungs had interstitial lung disease in lobes distant from the upper zone on HRCT (5). Furthermore, 6/12 PPFE lungs had areas of consolidation and 1/12 had bronchiectasis. In the present study, HRCT identified “ground glass” opacity in 4/7 ‘PPFE-like’ lungs and traction bronchiectasis in all 7 lungs. The presence of bronchocentric consolidation in HRCT images

of 5 of these 7 lungs further supports the proposal that chronic airway disease could be key to PPFE pathogenesis (5). Bronchocentric changes were also evident histologically, with all 10 'PPFE-like' lungs having variable lymphoplasmacytic bronchiolitis, and 8/10 having areas of bronchocentric fibrosis. A patchy lymphoplasmacytic infiltrate was a feature of the PPFE cases reported by Frankel *et al*, 2004 (3), while Reddy *et al*, 2012 (5) found bronchocentric fibrosis in 11/12 PPFE cases, with all 12 cases having focal non-specific chronic inflammation with lymphoid follicle accumulation.

Other features of PPFE shared by donkey 'PPFE-like' lungs included perilobular fibrosis (10/10) and venous and arterial intimal fibrosis (9/10) (5, 11). Vascular changes in donkey lungs were considered to reflect secondary intimal invasion by the surrounding fibrosis, rather than a primary vasculopathy. While granulomatous inflammation is not a key accepted feature of PPFE, it has also been detected in PPFE cases (5) and was an additional feature of 3/10 'PPFE-like' lungs. However, mycobacteria and fungi were not identified in the granulomatous lesions. Pleural fibrosis is a feature of asbestos-induced pulmonary fibrosis (12) in humans. Inorganic fibre content of the *ex vivo* donkey lung tissue was minimal and there was no evidence of asbestos fibres. The presence of non-fibrous dust particles such as calcium silicate was unsurprising considering the grazing habits of donkeys and likely reflected local soil composition. Potential toxicity of calcium silicate is thought to be minimal (13) and the dust burden of *ex vivo* donkey tissue was not considered to be significant.

The significance of elastosis within fibrotic donkey tissue is unclear. Elastosis and upregulation of elastin gene expression occurs in a murine model of pulmonary fibrosis (14), and in humans, progressive vascular fibroelastosis occurs in idiopathic interstitial pneumonias and correlates with a poor prognosis in usual interstitial pneumonia (15). An overall increase in both collagen and elastin with alveolar septal elastosis has been documented during the late phase of adult respiratory distress syndrome and in usual interstitial pneumonia (16).

Reddy *et al*, 2012, reported that 7/12 PPFE patients had a history of recurrent lower respiratory tract infections, leading the authors to postulate the contribution of such infections to the pathogenesis of PPFE (5). Further investigation is required to determine whether donkeys with PPFE-like disease had preceding recurrent lower respiratory tract infections (Supplemental data and e-Table 1).

In the horse, a progressive fibrosing interstitial lung disease termed Equine Multinodular Pulmonary Fibrosis (EMPF) is associated with equine herpesvirus 5 infection (17). Similarly asinine herpesvirus 4 and 5 (AsHV-4, AsHV-5) were implicated in an acute fibrosing interstitial pneumonia in 11 donkeys in North America and in a pyogranulomatous pneumonia in a mare (8, 18). Kleiboeker *et al*, (2002) described multifocal to coalescing nodules of fibrosis scattered throughout the lung parenchyma in the most severely affected of the 11 donkeys, a pattern similar to that seen in EMPF and quite different to the pathology described herein for DPF. Kleiboeker *et al* (2002) also detected herpesviral DNA in lung homogenate in all 11 affected donkeys but not in 6 control animals (8). This differs from the current findings that lung homogenates from all DPF and control donkeys were positive for AsHV-4 or-5. The role of AsHV-4 and -5 in DPF warrants further study.

In conclusion, over 50% of donkeys with DPF in this study shared key imaging and pathological characteristics of human PPFE, a rare and usually idiopathic interstitial pneumonia (4). Hence the donkey may provide a unique progressive model in which to study PPFE. The ubiquitous presence of gamma herpesvirus in the study population of donkeys warrants further investigation with regard to its potential role in the aetiology of DPF.

Acknowledgements

Author Contributions: A.Miele, collected data and wrote manuscript; K.Dhaliwal, study concept, overall guidance and wrote manuscript; N. Du Toit, tissue collection and intellectual contributions; J.Murchison described, assessed and scored imaging data, intellectual contributions; C.Dhaliwal, scored histology data and intellectual contributions; H.Brooks, tissue collection and intellectual contributions; S.Smith, described histology and intellectual contributions; N.Hirani, intellectual contributions; T.Schwarz, performed HRCT and intellectual contributions; C.Haslett, intellectual contributions; W.Wallace described, assessed and scored histology data, intellectual contributions; B.McGorum study concept, overall guidance and wrote manuscript.

Conflict of Interest: The authors have no conflict of interest to declare.

Other Acknowledgments: The authors thank Dr R. Dalziel, The Roslin Institute and R(D)SVS , University of Edinburgh, for performing DNA extraction and herpesviral PCR, Dr. A. R. Gibbs, Environmental Lung Disease Research Group, University Hospital Llandough, Penarth, for performing xray diffraction analysis, and the Clinical Research Imaging Centre, University of Edinburgh for conducting HRCT scans.

References

1. Chua F, Gauldie J, Laurent GJ. Pulmonary fibrosis: Searching for model answers. *Am J Respir Cell Mol Biol.* 2005;33:9-13.
2. Williams K, Malarkey D, Cohn L, et al. Identification of spontaneous feline idiopathic pulmonary fibrosis. *Chest.* 2004;125:2278-2288.
3. Frankel SK, Cool CD, Lynch DA, et al. Idiopathic pleuroparenchymal fibroelastosis; description of a novel clinicopathologic entity. *Chest.* 2004;126:2007-2013.

4. Travis WD, Costabel U, Hansell DM, et al. An Official American Thoracic Society/European Respiratory Society Statement: Update of the International Multidisciplinary Classification of the Idiopathic Interstitial Pneumonias. *Am J Respir Crit Care Med.* 2013;188:733-748.
5. Reddy TL, Tominaga M, Hansell DM, et al. Pleuroparenchymal fibroelastosis: A spectrum of histopathological and imaging phenotypes. *Eur Respir J.* 2012;40:377-385.
6. Morrow L, Smith K, Piercy R, et al. Retrospective analysis of post-mortem findings in 1,444 aged donkeys. *J Comp Pathol.* 2010;144:145-156.
7. Williams K, Derksen F, de Feijter-Rupp H, et al. Regional pulmonary veno-occlusion: A newly identified lesion of equine exercise-induced pulmonary hemorrhage. *Vet Pathol.* 2008;45:316-326.
8. Kleiboeker SB, Schommer SK, Johnson PJ, et al. Association of two newly recognized herpesviruses with interstitial pneumonia in donkeys (*Equus asinus*). *J Vet Diagn Invest.* 2002;14:273-280.
9. McLaughlin Jr RF, Tyler WS. Subgross pulmonary anatomy in various mammals and man. *JAMA:* 1961;175:694-697.
10. Thiemann A, Bell N. The peculiarities of donkey respiratory disease. *LEKEUX, P Equine respiratory disease. International Veterinary Information Service* [serial online] 2001 [sited 2001 Nov 14]. Available from www.ivis.org/special_books/Lekeux/bell/ivis.pdf.
11. Piciucchi S, Tomassetti S, Casoni G, et al. High resolution CT and histological findings in idiopathic pleuroparenchymal fibroelastosis: Features and differential diagnosis. *Respir Res.* 2011;12:111.
12. Bergin C, Castellino R, Blank N, et al. Specificity of high-resolution CT findings in pulmonary asbestosis: Do patients scanned for other indications have similar findings? *AJR Am J Roentgenol.* 1994;163:551-555.

13. Bolton R, Addison J, Davis J, et al. Effects of the inhalation of dusts from calcium silicate insulation materials in laboratory rats. *Environl Res.* 1986;39:26-43.
14. Hoff CR, Perkins DR, Davidson JM. Elastin gene expression is upregulated during pulmonary fibrosis. *Connect Tissue Res.* 1999;40:145-153.
15. Parra ER, Kairalla RA, de Carvalho CRR, et al. Abnormal deposition of collagen/elastic vascular fibres and prognostic significance in idiopathic interstitial pneumonias. *Thorax.* 2007;62:428-437.
16. Negri E, Montes G, Saldiva P, et al. Architectural remodelling in acute and chronic interstitial lung disease: Fibrosis or fibroelastosis? *Histopathology.* 2000;37:393-401.
17. Williams K, Maes R, Del Piero F, et al. Equine multinodular pulmonary fibrosis: A newly recognized herpesvirus-associated fibrotic lung disease. *Vet Pathol.* 2007;44:849.
18. De Witte FG, Frank N, Wilkes R, et al. Association of Asinine Herpesvirus - 5 with pyogranulomatous pneumonia in a mare. *J Vet Intern Med.* 2012;26:1064-1068.

Table 1: Classification of *ex vivo* donkey lungs

Case No.	Imaging Type	Imaging Classification	Histology Classification	Overall Classification
1	HRCT	Inconsistent	Inconsistent	Inconsistent
2	HRCT	Consistent	Inconsistent	Inconsistent
3	HRCT	Consistent	Consistent	Consistent
4	HRCT	Consistent	Consistent	Consistent
5	HRCT	Consistent	Consistent	Consistent
6	HRCT	Consistent	Consistent	Consistent
7	HRCT	Consistent	Consistent	Consistent
8	HRCT	Inconsistent	Inconsistent	Inconsistent
9	HRCT	Consistent	Consistent	Consistent
10	HRCT	Consistent	Consistent	Consistent
11	Digital	Inconsistent	Inconsistent	Inconsistent
12	HRCT	Consistent	Inconsistent	Inconsistent
13	Digital	Consistent	Consistent	Consistent
14	Digital	Consistent	Inconsistent	Inconsistent
15	Digital	Consistent	Inconsistent	Inconsistent
16	Digital	Consistent	Consistent	Consistent
17	Digital	Consistent	Inconsistent	Inconsistent
18	Digital	Consistent	Consistent	Consistent

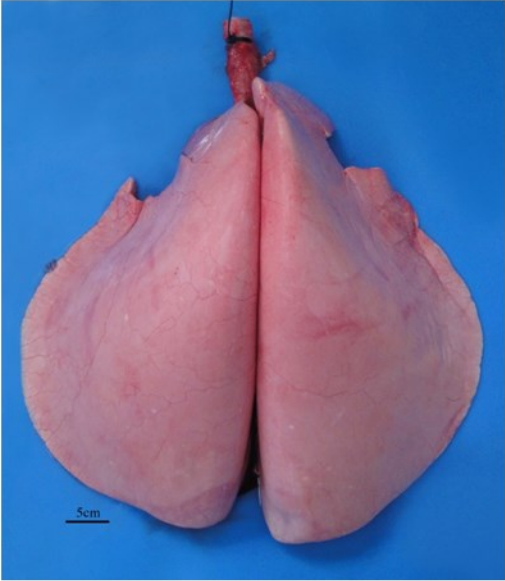
19	Digital	Inconsistent	Inconsistent	Inconsistent
----	---------	--------------	--------------	--------------

Table 2: Frequency of imaging and histological features identified in *ex vivo* ‘PPFE-like’ donkey lungs

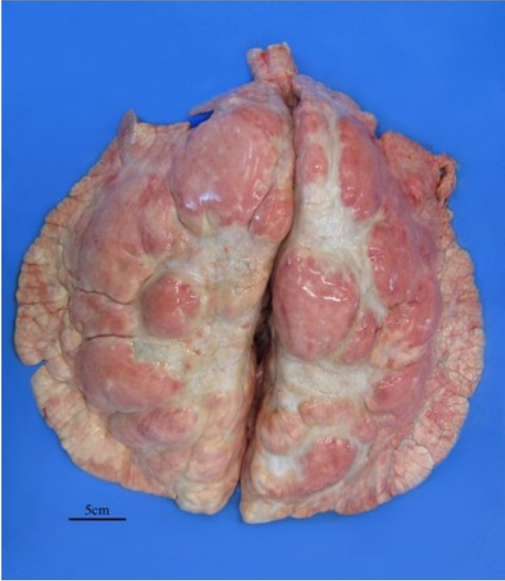
Imaging (digital and HRCT)		Histology	
Feature	Frequency	Feature	Frequency
Pleuroparenchymal thickening predominant in upper zones	10/10	Pleural and subpleural fibrosis with intra-alveolar fibrosis and elastosis in dorsal lung sections	10/10
Subpleural fibrosis	10/10	Inter-lobular septal fibrosis	10/10
Ventral fibrosis	7/10	Bronchocentric fibrosis	8/10
Parenchymal bands	7/7	Lymphoplasmacytic bronchiolitis	10/10
Traction bronchiectasis	7/7	Venous and arterial intimal fibrosis	9/10
“Ground glass” opacity	4/7	PPFE pattern in ventral lobe biopsies	2/6
Bronchocentric consolidation	5/7	Granulomatous inflammation	3/10
		Pleural ossification/calcification	1/10

Figure 1: Photographs of the dorsal (uppermost) surface of inflated *ex vivo* control (A) and ‘PPFE-like’ (B) lungs. Where HRCT was not available, lungs were sectioned vertically prior to digital imaging (C). Note the extensive dorsal pleural fibrosis in (B) and (C).

A



B



C

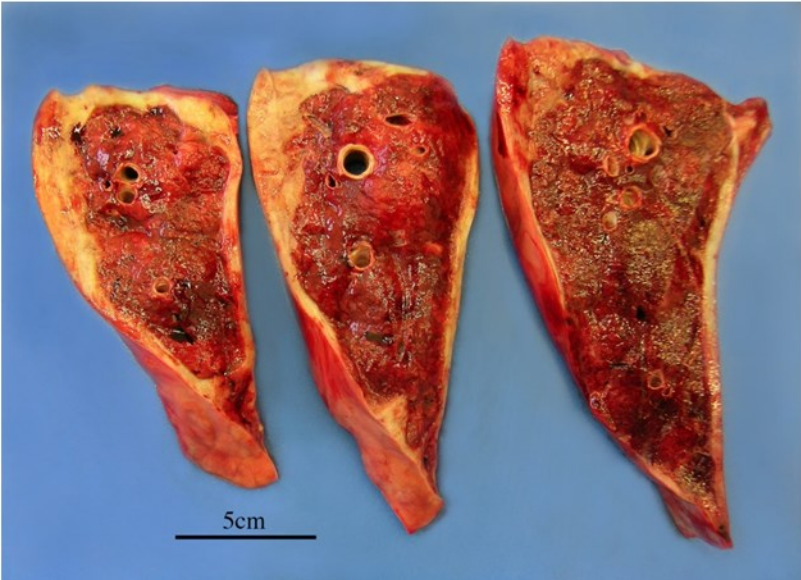
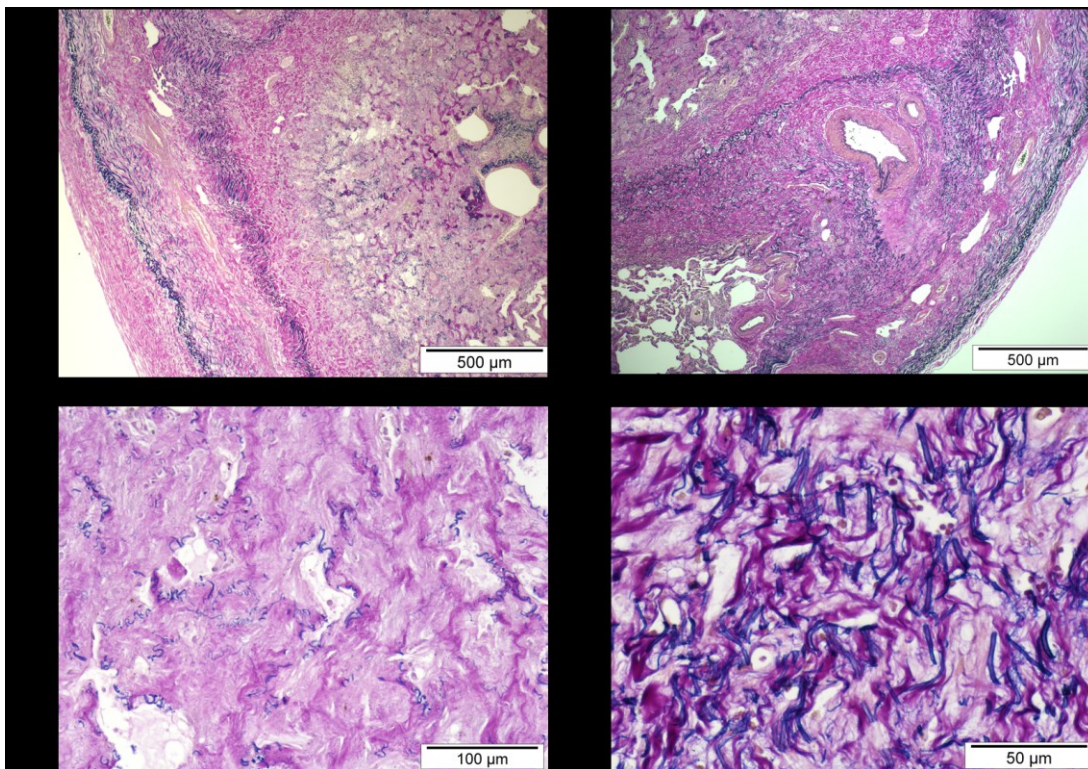


Figure 2: (A-H) Histology images of sections from ‘PPFE-like’ donkey lungs. (A) Pleural and subpleural fibrosis with alveolar septal elastosis and intra-alveolar fibrosis, EVG. (B) Disarray of the pleural elastin with a band of fibrosis extending from the subpleura along an interlobular septum, EVG. (C) Higher powered view of an area of intra-alveolar fibrosis, EVG. (D) High power view of an area of diffuse elastosis, EVG. Other common histological features of the ‘PPFE-like’ *ex vivo* donkey lungs include spatial heterogeneity (E) EVG, aggregates of mononuclear inflammatory cells (F) H&E, bronchiolocentric inflammation and fibrosis (G) H&E, and intimal fibrosis and elastosis of entrapped vessels (H) EVG. (I-J) Sections of DPF tissue classified as ‘inconsistent with’ PPFE, H&E, demonstrating intra-alveolar inflammation and fibrin deposition (I) and fibrosis of the alveolar walls with conservation of alveolar architecture (J).



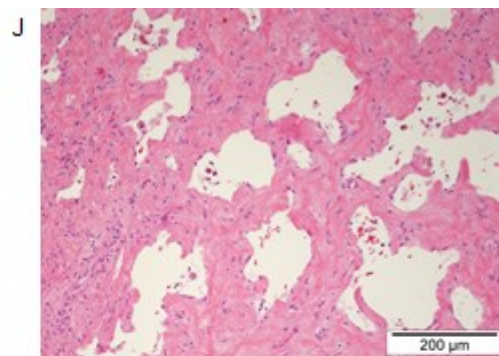
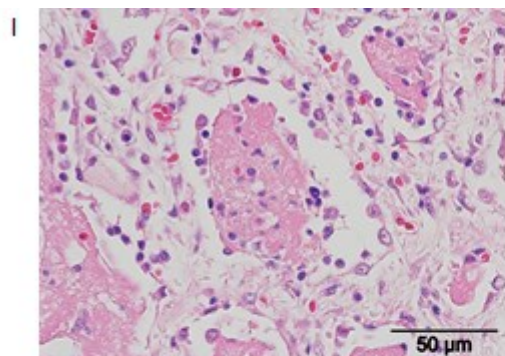
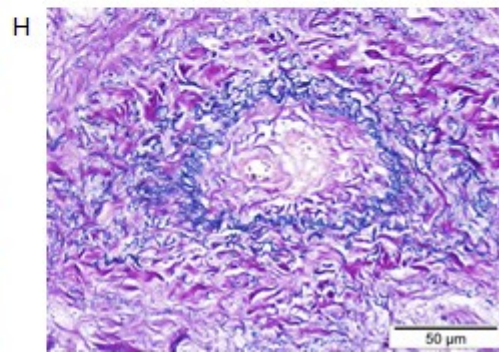
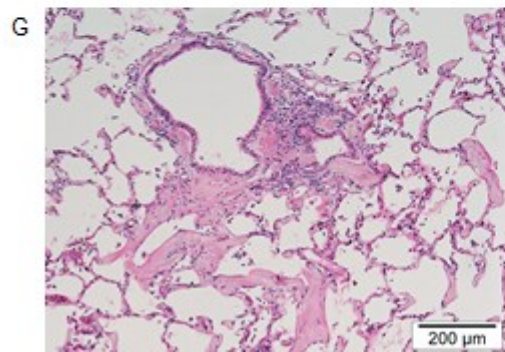
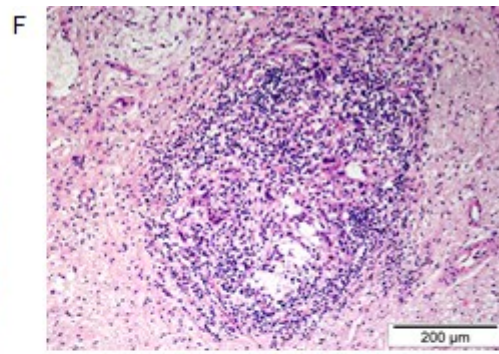
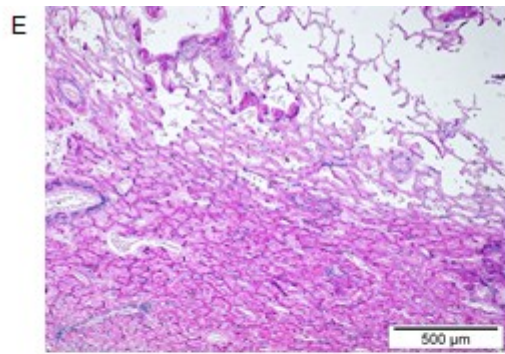


Figure 3: Cranio-caudal HRCT images of ‘PPFE-like’ inflated *ex vivo* donkey lungs.

Pathology ranged from mild dorsal pleural fibrosis extending along parenchymal bands (A) to thick rinds of pleural fibrosis encasing the dorsal surface of the lung (C). Also note the traction bronchiectasis (large arrow) and bronchocentric fibrosis (small arrow).

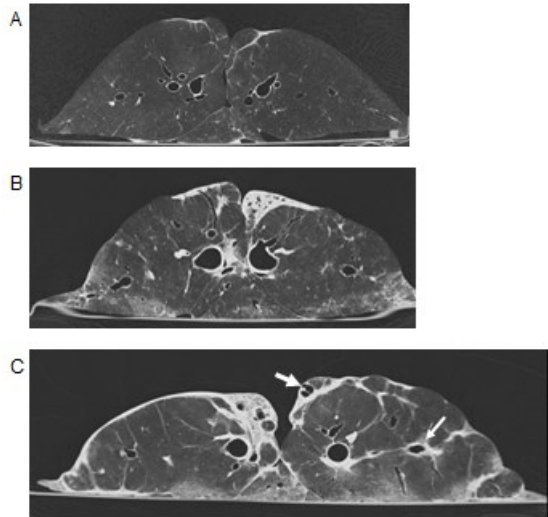


Figure 4: HRCT images of fibrotic inflated *ex vivo* donkey lungs classified as ‘inconsistent with’ PPFE on both imaging and histology. Images A-B show a predominantly ventral distribution to the fibrosis whereas image C demonstrates diffuse “ground glass” change.

